WHAT ARE THE OLIVINE-RICH BOULDERS IN THE UPPER FAN AND MARGIN UNIT AT JEZERO CRATER, MARS? O. Beyssac[1], E. Clavé[2], A. Udry[3], E. Dehouck[4], O. Forni[5], C. Quantin-Nataf[4], G. Lopez-Reyes[6], P. Beck[7], C. Royer[8], T. Gabriel[9], L. Kah[10], S. Schroeder[2], J.R. Johnson[11], T. Fouchet[12], J. Simon[13], A. Cousin[5], S. Maurice[5] & R.C. Wiens[8] [1]IMPMC, Paris, France (Olivier.Beyssac@upmc.fr); [2]DLR Berlin; Germany, [3]UNLV Las Vegas, USA; [4]LGLTPE Lyon, France; [5]IRAP Toulouse, France; [6]UVa, Valladolid, Spain; [7]IPAG Grenoble, France; [8]Purdue univ, Lafayette, USA; [9]USGS, USA; [10]Univ. of Tennessee, USA; [11]JHUAPL, USA; [12]LESIA, France; [13]JSC NASA, USA

Introduction: Since February 2021, the Perseverance rover has explored Jezero Crater in the Nili Fossae region of Mars which hosts large outcrops of a regional olivine-carbonate unit [1-3] . In the crater floor, Perseverance investigated two igneous formations [4-5]: Máaz, composed of basaltic lava and/or pyroclastic flows [6], and Séítah, an olivine-rich cumulate [7-8] below Máaz. Then, Perseverance explored the western fan composed by diverse sedimentary rocks [9] of variable composition, but often containing olivine [10] On the upper fan and margin unit, Perseverance encountered number of centimetric to metric boulder rocks [11]. Two main types of boulders were identified based on texture and composition: the olivine-rich and pyroxene-bearing [12] boulders. Here, we use SuperCam data to describe the texture, geochemistry and mineralogy of the olivine-rich boulders. Then, we discuss their possible petrological origin and some possible implications for the regional Nili Fossae olivine-carbonate unit.

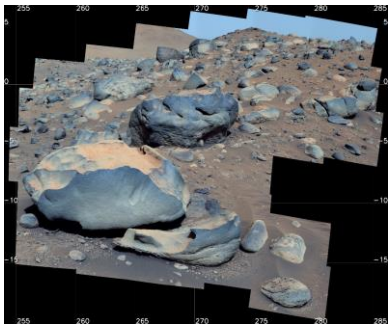

Figure 1: Mastcam-Z enhanced color mosaic showing a field of boulders in the upper fan on sol 800 (zcam08821).

The SuperCam instrument: SuperCam analyzes elemental chemistry by LIBS remotely (up to 7 m) and mineralogy by VISIR and Raman spectroscopy of the target [13-14]. It also provides high-resolution context images with a Remote Micro Imager (RMI) to describe the rock texture. LIBS provides a quantitative estimate of major elements present in the fraction of rock ablated by the laser within a ~350 µm wide spot [15], as well as (semi-)quantitative information on many light and/or minor elements, such as Cr, H or C. In some rocks, grains are larger than the LIBS spot size making possible single crystal analysis and stoichiometric analysis [6-7]. VISIR and Raman spectroscopy have a larger analytical footprint (in the mm range) and generally sample several grains.

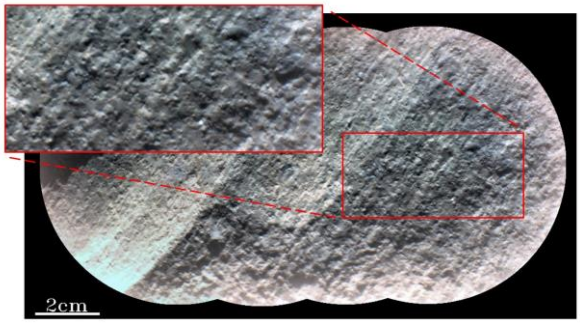

Figure 2: RMI image of sol 792 Mount Ida target showing the grainy texture.

Textures of the boulders: Most boulders were observed on the upper fan and in the Margin unit. They cover large areas and they appear as dark, massive, generally rounded rocks from some distance (Fig. 1). RMI reveal that these rocks are grainy and consist in the accumulation of millimetric grains against each other with no evident interstitial matrix (Fig. 2).

Bulk geochemistry: The olivine-rich boulders have an ultramafic composition: high MgO, moderate to high FeO, relatively low CaO, low Al_2O_3 and alkali. This composition bears some similarity with that of the Séítah rocks, but boulders show consistently higher bulk Mg# (molar 100xMgO/(MgO+FeO), lower CaO and Al_2O_3 (Fig. 3). Moreover, the carbonates locally observed in Séítah [16] are rarely detected in the boulders.

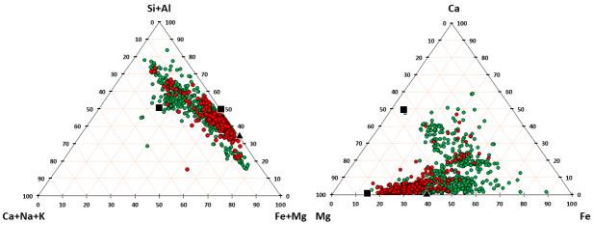

Figure 3: Si+Al – K+Ca+Na – Fe+Mg and Ca – Mg – Fe ternary diagrams with olivine-rich boulders (red) and Séítah (green). Triangle and square are onboard olivine and pyroxene standards

Mineralogy: Raman spectroscopy has been performed only once on an abraded patch of a boulder (sol 853, Lake Haiyaha target), yet the spectrum shows

strong olivine detection with the characteristic doublet at ~820 and ~850 cm^{-1} (Fig. 4). Using the relevant calibration [17-18], it is possible to estimate the forsterite (Fo)# of 70–72 for this olivine based on Raman data. VISIR spectra (Fig. 5) show a strong red slope in the 1.3 to 1.7 µm range with a downturn indicative of a ferrous phase consistent with olivine. Some spectra exhibit additional features at ~1.9 µm (H_2O) and a ~2.3 µm band related to either Fe/Mg-OH or carbonates. The latter is suggested when the ~2.3 um band is paired with a ~2.5 µm band. Based on these techniques, the rocks preserve strong signature from primary minerals and secondary phases are rare mostly consisting in Fe/Mg-rich clays and rare carbonates.

Most LIBS points are clustered close to the olivine reference with a slight trend showing some mixture with low-Ca pyroxene. Many LIBS points are consistent with analysis of pure olivine grains with Fo# 70-80 in agreement with PIXL [19]. Two points have composition consistent with pure orthopyroxene with high Mg# around 75. In general, H scores for LIBS points are low, suggesting that these rocks are relatively anhydrous. Many LIBS points show strong Cr peaks at ~425.5 and ~427.5 nm associated with high FeO and often high TiO_2, indicating the presence of Fe-Cr-(Ti)-rich phases, such as chromite or Cr-rich ulvöspinel.

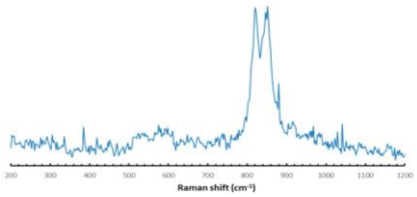

Figure 4: Raman spectrum (average of all points) for sol 853 Lake Haiyaha target showing the presence of olivine.

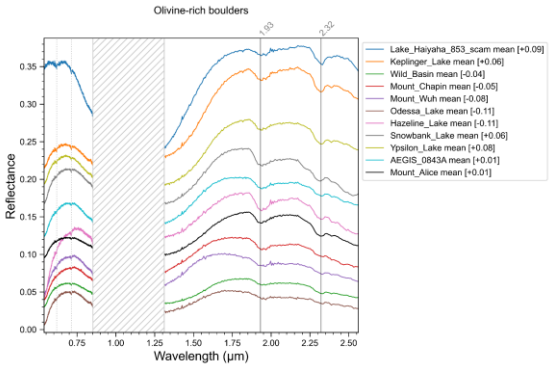

Figure 5: representative IR spectra for the olivine-rich boulders, with offsets shown in legend.

Interpretation: Texture and composition strongly favor an igneous origin for the olivine-rich boulders. These rocks have an ultramafic composition, remarkably homogeneous for some targets, largely dominated by olivine with Fe-Cr-(Ti)- phases (chromite or ulvöspinel) and minor low-Ca pyroxene. The boulders are only weakly altered and preserve magmatic textural and compositional information. Olivine Fo# are in the range of the bulk rock Mg# suggesting that they are not at equilibrium: this is likely the consequence of local olivine accumulation. As in Séítah, these rocks are an olivine-rich cumulate, yet there are some differences in composition. The boulders have actually a less evolved composition compared to Séítah: higher bulk Mg# and olivine Fo#, more olivine and less pyroxene with no evidence of high-Ca pyroxene. This composition bears some similarity with olivine-phyric- and poikilitic- shergottites [20] and, overall, with the Northwest Africa NWA 2737 chassignite [21], which is a dunite and has one of the less evolved composition among martian meteorites.

Conclusion: The olivine-rich boulders are olivine cumulates with a primitive composition. They could represent the less evolved fraction of the Séítah cumulate series, although they are found at much higher elevation compared to Séítah in the stratigraphy. Future petrological modeling will be done to test this hypothesis. Alternatively, they could represent the first *in situ* detection of martian mantle rocks since their texture and composition are consistent with terrestrial dunite, and their bulk Mg# is close to the estimated martian mantle Mg# [22].

The olivine-rich boulders likely originate from outcrops of the regional olivine-carbonate outcrops in the Neretva river catchment and were transported in the fan likely during catastrophic floods [23]. All these boulders carry some information for the provenance and stratigraphy [24-25]. The significant compositional difference with Séítah suggests that this regional unit is not homogeneous in composition and may not be uniform in nature.

Acknowledgments: The Mars2020 team is thanked for its generous contributions to this work. This work was supported by CNES in France and by the Mars Exploration Program in the US.

References: [1] Hoefen et al., Science 2003; [2] Horgan et al., Icarus 2020; [3] Mandon et al., Icarus 2020; [4] Farley et al., Science 2022; [5] Wiens et al., Sciences Advances 2022; [6] Udry et al., JGR Planets 2023; [7] Beyssac et al., JGR Planets 2023; [8] Liu et al., Science, 2022; [9] Stack et al., LPSC 2023; [10] Dehouck et al., LPSC 2023; [11] Vaughan et al., LPSC 2024; [12] Dehouck et al., LPSC 2024; [13] Wiens et al., SSR 2021; [14] Maurice et al., SSR 2021; [15] Anderson et al., SAB 2022; [16] Clavé et al., JGR Planets 2023; [17] Kuebler et al., GCA 2006; [18] Lopez-Reyes et al., subm.; [19] Moreland et al., LPSC 2024; [20] Udry et al., JGR Planets 2020; [21] Beck et al., EPSL 2006; [22] Yoshizaki & McDonough GCA 2020; [23] Mangold et al., Science 2021; [24] Gwizd et al., LPSC 2023; [25] Canciolo et al., LPSC 2023.